Promoting Uranium Immobilization by the Activities of Microbial Phosphatases

Robert J. Martinez[1], Melanie J. Beazley[2], Martial Taillefert[2] and Patricia A. Sobecky[1]

[1]School of Biology, Georgia Institute of Technology, Atlanta Georgia and [2]School of Earth and Atmospheric Sciences, Georgia Institute of Technology, Atlanta Georgia

Abstract

The treatment of hazardous waste sites, particularly those containing metals and radionuclides, remains one of the most costly environmental challenges currently faced by the U.S. and other countries. A potential approach to the immobilization and/or sequestration of these hazardous wastes is the use of nonspecific phosphohydrolases (i.e., acid phosphatases) in naturally occurring subsurface microbial populations to promote the immobilization of radionuclides through the production of metal phosphate precipitates. Nonspecific acid phosphohydrolases are a broad group of secreted microbial phosphatases that function in acidic-to-neutral pH ranges and utilize a wide range of organophosphoester substrates. We have previously shown that PO_4^{3-} accumulation during growth on a model organophosphorus compound was attributable to the overproduction of alkaline phosphatase by genetically modified subsurface pseudomonads. In the present study, we have extended these results to indigenous metal resistant subsurface microorganisms cultivated from the Field Research Center (FRC), Oak Ridge Tennessee. The analysis of a subset of gram positive FRC isolates cultured from radionuclide and metal contaminated FRC soils and uncontaminated (control) sediments indicated a higher percentage of isolates exhibiting phosphatase phenotypes (i.e., in particular those surmised to be PO_4^{3-}-irrepressible) relative to isolates from the background reference site. A high percentage of strains which exhibited such putatively PO_4^{3-}-irrepressible phosphatase phenotypes were also shown to be resistant to the heavy metals lead and cadmium. A *Rhanella* sp., Y9, from the FRC collection has been shown to facilitate the precipitation of uranium from solution. We are presently conducting PCR-based detection and

Image from http://public.ornl.gov/nabirfrc/photos_history.cfm

Hypotheses to be tested:

(1). Non-specific phosphophydrolases (acid phosphatases) provide subsurface microorganisms with resistance to heavy metals and lateral gene transfer has promoted the dissemination of this phosphatase-mediated resistance.

(2). Phosphatase activities of the subsurface bacterial populations can promote the immobilization of radionuclides via the formation of insoluble metal phosphate precipitates.

(3). Subsurface geochemical parameters (pH, nitrate) will affect phosphate mineral formation by altering microbial phosphatase activity and/or affecting the stability of the metal phosphate precipitates.

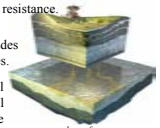

Image from: http://www.inel.gov/initiatives/subsurface.shtml

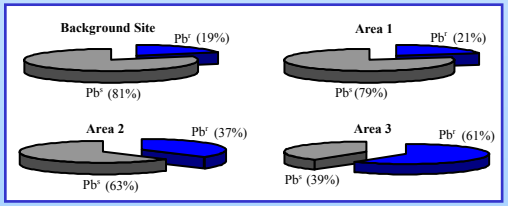

Figure 1. Lead [Pb(II)] resistance screening of FRC isolates from Areas 1, 2, 3 and the reference background site. Isolates cultured from Area 3 exhibited the highest incidence (61%) of Pb(II) resistance relative to Areas 1, 2 and the background site.

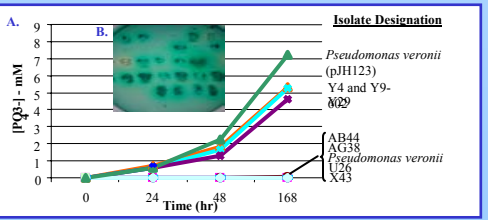

Figure 2. (A) Phosphate liberation of select FRC isolates which were identified as Pb^{r}and exhibiting cell surface and/or extracellular phosphatase activity. FRC isolates assayed for phosphate liberation were obtained from the background reference site (AG38), Area 2 (AB44) and Area 3 (U26, X43, Y4, Y9-602 and Y29). A subsurface *Pseudomonas veronii* V1 isolate from Subsurface Microbial Culture Collection (SMCC) harboring the constitutive phoA plasmid pJH123 and the plasmid free *Pseudomonas veronii* V1 host were used as positive and negative controls for phosphatase activity, respectively. **(B)** Tryptose Phosphate Methyl Green (TPMG) agar plates were used to screen for phosphatase phenotypes. Phosphatase positive phenotypes appear as dark green colonies and/or cause the surrounding medium to darken. Negative phenotypes appear unstained.

Table 1: Cell viability after 1 hour expose to 200 µM uranyl acetate

Genus	Strain Designation	CFU (washed)	CFU (without 200µM U)	CFU (with 200µM U)	Reference
Arthrobacter	FRC-AA1	$1.79{\cdot}10^8 \pm 0.24$	$1.59{\cdot}10^8 \pm 0.25$	$1.45{\cdot}10^8 \pm 0.24$	This work
	FRC-AA21	$1.53{\cdot}10^8 \pm 0.18$	$7.78{\cdot}10^7$	$6.45{\cdot}10^7 \pm 0.19$	This work
	FRC-AA25	$2.31{\cdot}10^8$	$1.39{\cdot}10^8$	$9.20{\cdot}10^7 \pm 0.24$	This work
	FRC-V45	$1.67{\cdot}10^8 \pm 0.20$	$9.13{\cdot}10^7$	$6.85{\cdot}10^7$	This work
	FRC-X34	$1.83{\cdot}10^8$	$1.71{\cdot}10^8$	$1.07{\cdot}10^8$	This work
	S3Y	$5.10{\cdot}10^9$	$7.25{\cdot}10^9$	$6.45{\cdot}10^7$	(Suzuki & Banfield, 2004)
	W1	$1.98{\cdot}10^{10}$	$1.98{\cdot}10^{10} \pm 0.24$	$2.17{\cdot}10^{10}$	(Suzuki & Banfield, 2004)
	A. histidinolovorans	$1.57{\cdot}10^8$	$6.10{\cdot}10^7 \pm 0.25$	$4.35{\cdot}10^7 \pm 0.51$	This work
Rhodococcus	S7S	$1.92{\cdot}10^9 \pm 0.24$	$2.28{\cdot}10^9 \pm 0.34$	$1.43{\cdot}10^9$	(Suzuki & Banfield, 2004)
Bacillus	FRC-N65	$2.99{\cdot}10^8$	$1.12{\cdot}10^8 \pm 0.19$	$<1{\cdot}10^4$	This work
	FRC-X18	$1.87{\cdot}10^8 \pm 0.25$	$3.51{\cdot}10^7 \pm 0.57$	$4.03{\cdot}10^5$	This work
	FRC-Y9-2	$2.55{\cdot}10^7 \pm 0.32$	$3.12{\cdot}10^6 \pm 0.53$	$<1{\cdot}10^4$	This work
	S1	$4.56{\cdot}10^8$	$<3{\cdot}10^6$	$<3{\cdot}10^6$	(Suzuki & Banfield, 2004)
	S2	$1.54{\cdot}10^8 \pm 0.25$	$<3{\cdot}10^6$	$<3{\cdot}10^6$	(Suzuki & Banfield, 2004)
	B. cereus	$9.70{\cdot}10^7 \pm 0.26$	$<1{\cdot}10^4$	$<1{\cdot}10^4$	This work
Escherichia	*E. coli* JM109	$8.00{\cdot}10^7 \pm 0.19$	$4.65{\cdot}10^7 \pm 0.15$	$<1{\cdot}10^4$	This work
Rahnella	FRC-Y9-602	$1.10{\cdot}10^8$	$5.40{\cdot}10^7 \pm 0.20$	$1.54{\cdot}10^6 \pm 0.46$	This work

Cell viability assays were done to determine FRC isolate tolerances to 200 µM uranyl acetate. Both *E. coli* JM109 and FRC strains were grown to mid-log phase in Lennox Broth and Tryptic Soy Broth, respectively at 30°C. Cells were then washed twice in 0.1M NaCl pH 4. After last wash cells were: **1)** Diluted and plated to determine number of viable cells used for assay, **2)** Incubated for 1 hour in 0.1M NaCl pH 4 and **3)** Incubated 1 hour in 0.1M NaCl pH 4 containing 200 µM uranyl acetate. After 1 hour incubations, cells were diluted in 0.85% NaCl, plated on agar plates containing the same media used for liquid innoculations.

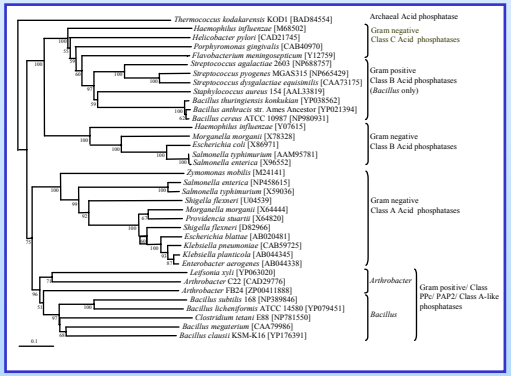

Figure 3. Neighbor-joining analysis of putative and functional acid phosphatases derived from completed genomes. Phlyogenetic relationship among the 3 characterized acid phosphatase groups is depicted in the rooted tree. Scale bar represent 0.1 changes per amino acid position. Alignments generated for each class of acid phosphatase proteins were used to generate phylum-specific PCR primers. Phylum-specific primers will be used to determine lateral gene transfer of acid phosphatases in FRC cultured isolates.

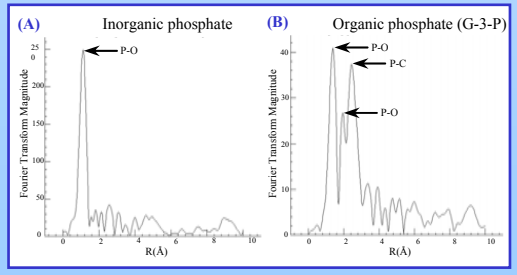

Figure 4. Preliminary EXAFS analysis of basal salts growth medium (BSM). **(A)** Analysis of BSM containing 100 mM inorganic phosphate. **(B)** Analysis of BSM containing 100 mM glycerol-3-phosphate (G-3-P). Data provided by Paul Northrup (Brookhaven National Laboratory).

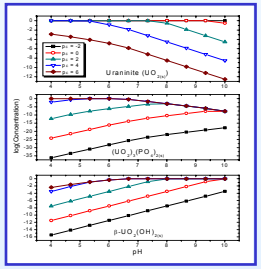

Figure 5. Concentrations of uraninite and the prevalent uranium phosphate and uranium hydroxide minerals found at equilibrium as a function of pH and pε in a typical contaminated groundwater containing U_T = 50 µM; ΣPO_4^{3-} = 40 µM; ΣCO_3^{2-} = 500 µM. At log (Concentration) = 0, the mineral precipitates. Dissolved uranium is essentially non-existent at pH < 7 at all pεs. At high pε and high pH, a maximum of 10% is found in solution as an $UO_2(HPO_4)_2^{2-}$ complex. From these calculations, low pH and high pε favor precipitation of uranium phosphate, high pH and low pε favor precipitation of uranium hydroxides, while a low pε favors precipitation of uraninite.

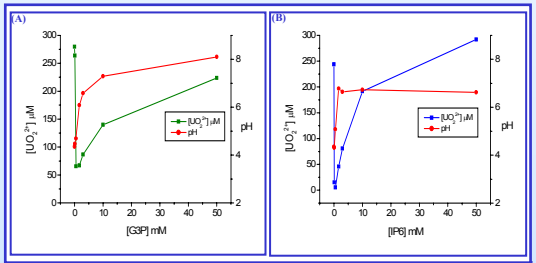

Figure 6A-6B. Solubility of U(VI) as a function of **(A)** G3P and **(B)** IP6 after 24 hour abiotic equilibration. Solubility of U(VI) in G3P decreases sharply between 0.1 and 0.5 mM G3P and then increases at high concentrations. U(VI) is highly insoluble at low concentrations of IP6 and precipitates completely. At higher concentrations of IP6 the solubility of U(VI) is enhanced, possibly due to increased repulsive negative charges around the uranyl ion. U(VI) analysis by laser-induced fluorescence (LIF) with pyrophosphate/hypophosphite reagent. Excitation at 395 nm and emission at 500 nm. Minimum detection limit 0.5 to 2 µM depending on medium. Sample solutions contain 300 µM uranyl acetate and 10 mM glycerol in a basal salts media (BSM). IP6 was added in a 1.6:3.4 ratio of phytic acid:Na-phytic acid to provide a slightly acidic solution.

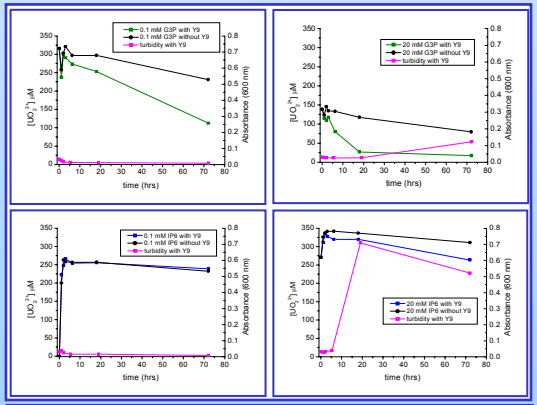

Figure 7A-7B. Kinetic study of U(VI) bioprecipitation in solutions containing isolate Y9-602 with G3P and IP6 as phosphate sources. All solutions contained 10 mM glycerol as a carbon source and 300 µM uranyl acetate in BSM medium. Samples were equilibrated for 24 hours and filtered (0.2 µM pore size) before adding Y9-602. At time 0, Y9-602 was added and the samples incubated for 72 hours at 30°C. Control samples without Y9-602 demonstrate the abiotic precipitation of U(VI). **(A)** After 72 hours in 0.1 mM G3P, 37.7% more U(VI) was precipitated biologically compared to the chemical control. **(B)** In 20 mM G3P, 87.5% of U(VI) was precipitated in the Y9-602 sample and 42.5% abiotically removed in the control, resulting in a 45.0% increase in biotic precipitation. **(C)** Due to 100% abiotic precipitation at time 0 in the 0.1 mM IP6 samples, a second amendment of 300 µM uranyl acetate was needed. After 72 hours, only 12% U(VI) was precipitated with little difference between the biotic and abiotic samples, indicating most of the IP6 had been removed prior to addition of Y9-602. **(D)** In 20 mM IP6, 17.5% more U(VI) was precipitated biologically compared to the abiotic control. U(VI) was least soluble in 20 mM G3P **(B)** and 0.1 mM IP6 **(C)** with 54% and 100% abiotic precipitation, respectively, before adding Y9-602.

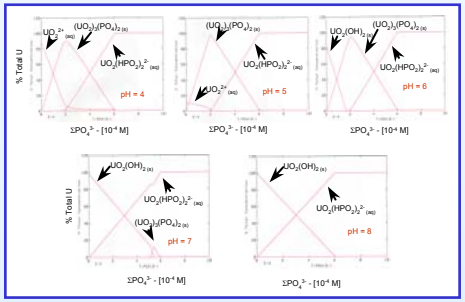

Figure 8. U(VI)-phosphate speciation at equilibrium predicted by MINEQL+ as a function of phosphate concentration in solution and pH . At low pH and low phosphate concentration, uranium is mainly under the form of uranyl ions. As the concentration of phosphate approaches that of total uranium, highly insoluble uranium phosphate compounds are formed. In excess phosphate, speciation calculations predict dissolution of this mineral and formation of uranium phosphate complexes in solution. At higher pH, uranium tends to be insoluble at low concentration of phosphate and soluble, as uranium phosphate complexes, at high phosphate concentration. The solid phase preferentially formed at pH > 7 is a uranium hydroxide mineral. These calculations were performed in the absence of carbonate species to illustrate the effect of phosphate on uranium speciation. Addition of carbonate does not change the behavior of uranium and phosphate.

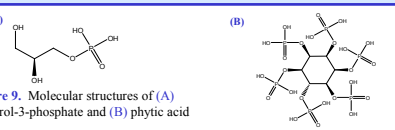

Figure 9. Molecular structures of **(A)** glycerol-3-phosphate and **(B)** phytic acid (IP6).

Conclusions

•Preliminary testing of a subset of lead-resistant subsurface isolates indicate a higher percentage of strains exhibiting phosphatase phenotypes from contaminated soils relative to isolates obtained from uncontaminated soils.

•To date, the majority of the lead-resistant, phosphatase positive isolates obtained from the FRC contaminated soils are Gram-positive *Bacillus* and *Arthrobacter* species.

•Preliminary testing indicates that the FRC isolate (Y9-602) has an enhanced tolerance to uranyl acetate when compared to the *E.coli* K12 strain JM109.

• Kinetic studies were conducted in solutions containing the Y9-602 isolate and an organo-phosphate compound to determine if the phosphatase activity of Y9-602 would enhance the precipitation of uranium (Figure 7).

•For these incubations two organo-phosphate compounds with different chemical structures were chosen as the phosphate source to determine how efficiently Y9-602 can hydrolyze these compounds. Phytic acid (IP6) is a six-member carbon ring with six attached orthophosphate groups which can provide up to twelve coordinate binding sites. Glycerol-3-phosphate is probably a more labile compound with only one orthophosphate attached to a three carbon chain. At neutral pH both molecules are negatively charged providing reactive sites for cationic binding.

•Studies were run at 0.1 mM and 20 mM concentrations of IP6 and G3P to account for the fact that abiotic precipitation of UO_2^{2+} is highly dependent on the concentration of these organo-phosphate compounds in solution (Figure 6). The solubility of UO_2^{2+} increases significantly with IP6 concentration. At high concentrations of IP6 the repulsive negative charges of the phosphate oxygens may hinder the ability of the phosphate complexes to nucleate and precipitate (Figure 8), therefore increasing solubility. U(VI) demonstrates high solubility at the lowest concentration of G3P, a sharp decrease in solubility as G3P content is increased up to 0.5 mM, followed by an increase in solubility at high G3P concentration.

•The solubility of U(VI) in the presence of Y9-602 followed the results shown in Figure 7. After 72 hours at both concentrations of G3P there was 38 to 45% enhancement of U(VI) precipitation in the biotic assays compared to the chemical controls. Suggesting U(VI)-phosphate mineral bioprecipitation. The IP6 assays had little difference between the control and the biotic sample. After 72 hours there did appear to be a slight enhancement of U(VI) precipitation of 17% in the biotic assay possibly indicating a longer time needed for bioprecipitation to occur with less-labile compounds.

Future Directions

- Enrichment cultures, using phytic acid and other organo-phosphate substrates, will be developed to obtain additional Gram-positive and Gram-negative FRC isolates.
- Determine the uranium tolerance of FRC isolates demonstrating enhanced phosphatase activity.
- Molecular characterizations of non-specific acid phosphatases from select FRC isolates will be conducted to determine substrate range, enzyme activity, optimal pH and the specific class (i.e., class A, B or C) using PCR primer sets developed in this project.
- Analysis of microbial precipitated uranium mineral via EXAFS.
- Analyze cells incubated with uranyl acetate using X-Ray microscopy to determine localization (cell surface or intracellular) of the uranium mineral.

Acknowledgements

This research is supported by the Office of Science (BER), U.S. Department of Energy, Grant No. DE-FG02-04ER63906